Comparison of pharmacokinetics and biodistribution of doxorubicin loaded in PEGylated liposomes and a phospholipid-free small unilamilar vesicle

by
Wunan Zhang

B.Sc. Sichuan University, 2016

A THESIS SUBMITTED IN PARTIAL FULFILLMENT OF
THE REQUIREMENTS FOR THE DEGREE OF

MASTER OF SCIENCE
in
THE FACULTY OF GRADUATE AND POSTDOCTORAL STUDIES
(Pharmaceutical Sciences)

THE UNIVERSITY OF BRITISH COLUMBIA
(Vancouver)
September 2018

The following individuals certify that they have read, and recommend to the Faculty of Graduate and Postdoctoral Studies for acceptance, a thesis/dissertation entitled:

Comparison of pharmacokinetics and biodistribution of doxorubicin loaded in PEGylated liposomes and a phospholipid-free small unilamilar vesicle

submitted by Wunan Zhang in partial fulfillment of the requirements for

the degree of Master of Science

in Faculty of Pharmaceutical Sciences

Examining Committee:

Shyh-Dar Li
Supervisor

Judy Wong
Supervisory Committee Member

Abby Collier
Supervisory Committee Member

Adam Frankel
Additional Examiner

Additional Supervisory Committee Members:

Urs Hafeli
Supervisory Committee Member

Abstract

The thesis focuses on the development and characterization of an innovative phospholipid-free small unilamellar vesicle (PFSUV) for drug delivery. The optimal PFSUVs composed of Tween80/cholesterol (1/5 molar ratio) were fabricated by microfluidics, exhibiting a mean diameter of 60-80 nm. The PFSUVs displayed a single bilayer spherical structure, similar to that of a standard liposomal formulation. Doxorubicin could be actively loaded into the aqueous core of PFSUVs at a drug-to-lipid ratio of 1/20 (w/w) via an ammonium sulfate gradient, and was stably retained for 6 days when incubated in 50% serum. In the presence of serum, DOX loaded PFSUVs were internalized by EMT6 murine breast tumor cells 2-fold more efficiently compared to the serum-free conditions due to LDL endocytosis pathway, while PEGylated liposomal doxorubicin (PLD, DSPC/Chol/DSPE-PEG2000) displayed little cellular uptake in both conditions. The results suggest that serum component(s) triggered cellular internalization of the PFSUVs. As a result, the *in vitro* potency of PFSUVs-DOX against EMT6 cells was comparable as free DOX and was significantly increased compared to the PLD. In mice, PFSUVs-DOX displayed rapid clearance from the blood (<5 μg/mL at 2 h post injection), while the PLD showed significantly prolonged blood circulation with a blood level of 34 μg/ml in 2 days. After i.v. delivery, the PLD selectively accumulated in the liver (4-5 μg/g tissue), spleen (3-5 μg/g) and tumor (0.5-1.3 μg/g) with minimal uptake in other tissues. The PFSUVs-DOX displayed a distinct biodistribution pattern with a high liver uptake at 2 h (~15 μg/g). Relatively low but significant uptake of the PFSUVs-DOX in the spleen (3~4 μg/g) and tumor (1 μg/g) was measured from 2-48 h post injection. DOX delivered by the PFSUVs was mainly detected in the

hepatocytes and Kupffer cells evidenced by confocal microscopy. To the best of our knowledge, this is the first report showing SUVs containing a phospholipid-free bilayer could be formed using microfluidics, and a drug could be actively loaded into the aqueous core for liver-targeted delivery.

Lay Summary

Drug delivery systems were designed to help drug accumulate in different area in human. With these tools, drugs can either have stronger effects or become less toxic. So we designed a drug delivery system with a hole inside to carry drugs and help drugs accumulate in liver. With this tool we invented, we hope to improve therapy of liver disease.

Preface

This thesis is composed of one manuscript that will be submitted for publication. Details of the specific nature of the experiments and the scope of the thesis work were formulated in discussions between Dr. Shyh-dar Li and myself. During the study, I received training in cell culture from Dr. KKr. Viswanadham, in plate reader from Dr. Alex Smith, in confocal microscopy from Miss Bahira Hussein, in tissue sectionS for Dr. Zoe Zou and Rishi Somvanshi. The Cryo-TEM result was performed with the assistance of Dr. Jayesh Kulkarni. Development and analysis of all PFSUVs formulations, and all the subsequent *in vitro* experiments were performed by me**.** I wrote this thesis under the guidance of my supervisor Dr. Shyh-dar Li.

Table of Contents

List of Tables

List of Figures

List of Abbreviations

Abbreviation	Definition
AS	Ammonium sulfate
Chol	Cholesterol
CLSM	Confocal Laser scanning microscopy
CPP	Critical packing parameters
COX-2	Cyclooxygenase-2
Cryo-TEM	Cryo-transmission electron microscopy
CXB	Celecoxib
DMSO	Dimethyl sulfoxide
DOTAM	*N*-[1-(2,3-dioleoyloxy)propyl]-*N*,*N*,*N*-trimethylammonium chloride
DSPC	1,2-distearoyl-sn-glycero-3-phosphocholine
DSPE-mPEG$_{2000}$	1,2-distearoyl-sn-glycero-3-phosphatiylethanol-amine-N-[methoxy (polyethyleneglycol)-2000
EPR	Enhanced permeability and retention
EtOH	Ethanol
FBS	Fetal bovine serum
HBS	HEPES buffered saline
HEPES	4-(2-hydroxyethyl)-1-piperazineethanesulfonic acid
HLB	Hydrophilic lipophilic balance
IC_{50}	Half maximal inhibitory concentration
i.v.	Intravenous
NSAID	Nonsteroidal anti-inflammatory drug
PEG	Polyethyleneglycol
PFSUV	Phospholipid free small unilamellar vehicle
PFSUV-DOX	Phospholipid free small unilamellar vehicle with DOX loaded
PBS	Phosphate buffer saline
PLD	PEGlyated liposomal doxorubicin
SRBC	Sheep red blood cell
TFF	Tangential flow filtration
ZP	Zeta Potential

Acknowledgements

I would like to express my great gratitude to my supervisor Dr. Shyh-Dar Li whose great mentorship gave me every opportunity for self-development. He inspired me to pursue a scientific career. He is the person who taught me how to embrace the failure, deal with the drawbacks and improve myself. The time under his supervision is one of the most precious time I have ever experienced, inspired by creative idea and fancy techniques. He did not only help me design experiments, but also more importantly, gave me a chance to glimpse everything with a web of logic. He set a great example of how to be a professional scientist. I would also like to thank Dr. Abby Collier dedicated great amount of time in helping students even at the first time we met in pharmacokinetic courses where I accidentally missed the first class. I can't remember how many times I received warm help from her. I also really appreciated the help from Dr. Judy Wong who spent a huge amount of time to support my project including reading all the reference I mentioned in my first committee meeting and I am grateful for her questions which can always bring new perspective on my research. I also appreciate Dr. Urs Hafeli who show great supports and curiosity which make it quite joyful to talk with. I also want to thanks Dr. Harvey Wong as the chair of my committee meeting whose effort made the whole program went smoothly. I want to offer a big thanks to Dr. Karla Williams for agreeing to become my external examiner and come to my final defense. I would like to thank Dr. Adam Frankel for his great support of agreeing to be my external examiner at the last minutes. Besides, I am grateful for the help we get from Dr. Ujendra Kumar who showed great support in our tissue section. Also I appreciated Dr. Pieter Cullis who provided technique support in Cryo-TEM imaging.

During this project, my labmates gave me a lot of assistance. I would like to thank Dr. Roland Böttger. He gave me great lectures on UPLC, which compensate a great pity in my program. He also joined me with those unhealthy snacks in the middle of night after working. He made those long uneasy night much more entertained and I am happy I don't need to conduct experiments in this 'Hunting building' all alone. I want to thank Dr. Qin Zhu who showed great support in my study and provided precious advice on confocal imaging. It's a great pleasure to talk with her, not only about science, but also about travel. I want to thank Dr. KKr. Viswanadham who trained me in the cell culture. I want to thank Dr. Mehrdad Bokharaei who taught me how to inject tumor cell into mice. I want to thank Anne Nguyen who is one of the kindest people I have ever met and brought great light to my life. I also want to thank Nojoud AL Fayez who is always so gentle and considerable. She gave me great comfort and encourages and demonstrated a precautious attitude towards research that I can learn from. I am so joyful that I can have those two magnificent ladies as company who is willing to share my sorrow and happiness. I want to thank Rita Zhao who gave me a lot advice and help me settle down when I come here. I also met a lot of amazing undergraduate students who provided significant help to my program. I want to thank Geoff Sall who helped me settle the tangential flow filtration system at the beginning, Jessie Zhang who helped me get familiar with the strange foreign environment when I first come here, Suen Ern Lee who encouraged me a lot and indicated a strong willing to discuss academic topics which can sometimes unexpectedly gave me inspiration, Sukhdeep Jatana and Joseph Ho who played as important roles in our lab and helped us to organize the lab.

I also want to express my gratitude to those people indicated their enormous generosity and kindness in our faculty. I want to thank Zoe Zou, Rishi Somvanshi, Alex Smith and Bahira Hussein

who gave me great technique supports and trained me with different instruments. I want to thank Sunny Yang who provided me with a lot of precious advice on cell culture and help me with IncuCeyte®. I want to thank Jafar Hasbullah in Dr. Colin Ross lab who provided me with MTT assay method for cell viability study and gave me encourage all the time. I also need to thank Dr. Jayesh Kulkarni who helped me visualize my formulation using cry o-TEM method. I want to thank Sarah Humle and other MBF faculty who helped me with my animal study.

There are two more people I have to talk about in this faculty, Lennart Johannes Bohrmann and Alice Yu. I don't want to mention how many supports and encourages I have received from them because it has already been out of number and I am so arrogant to receive them as if they are granted. Still I have one trivial little thing that I must speak out. I don't think I can make it without them, so I sincerely thank them for being in my life.

Meanwhile, I also want to thank those friends those who cared, helped and supported in the last two years. I want to thank Alexandra Kerron who provided me great comfort and gave me the first Christmas miracle after a cursed trip. I want to thank Yitong Li, one amazing young pharmacists in Australia, to whom I want to express my deepest gratitude and love for fighting forward together even though we failed to meet in Argentina, separated by the cruel immigration office. I want to thank Zhixin Li, a talented strong female who teach me about resilience and toughness. She also recommended me with Graphpad Prism first time and the quality of my scientific graphs boosted significantly ever after. I want to thank Sammy Zheng for bringing board games and entertaining the stressful research life. I also want to thank Dr. Lian Li, whom I can proudly claim as my friend. He set a great example for my academic career and inspired me to dip into my research with precious

advice. I want to thank Yining Xu, the most skillful young scientist I have ever seen, who, as a big sister I never had, encouraged me to follow the dream. I also want to thank Jasmine Hao who helped me get rid of hideous shadows from the past.

I want to thank my mother, Xiaoling Zhang and my father, Bin Wu who showed unconditional support and encouraged me to be brave, be bold and be kind all the time. And at last I truly appreciate Lixi Feng for responding my prayer all the time. Her holiness bestowed her benign guidance and blessing which lit up the dim trek with a whole shinning galaxy.

Chapter 1: Phospholipid-free liposomes for drug delivery

1.1 Phospholipid-free liposomes

Liposomes are vehicles composed of phospholipids and cholesterol, containing bilayer structure that separates the inner aqueous core from the external phase. Liposomes are biodegradable and biocompatible with low toxicity and immunogenicity. Hydrophilic and lipophilic drugs can be both loaded into the aqueous core and the lipid bilayer, respectively. Liposomes are the most established and versatile drug delivery system with several products approved clinically [1-4].

Guillaume Bastiat et al. [5] reported that palmitic acid and cholesterol could be used as lipid components to form phospholipid-free liposomal vesicles (Fig.1.1). Melted palmitic acid molecules provide a nonpolar environment for solubilizing cholesterol, which straightens the fatty acid chains, promoting a molecular order compatible with the bilayer formation[6]. Similarly, non-ionic surfactants alone or with cholesterol have been shown an ability to form vesicles that could encapsulate hydrophilic compounds, suggesting the existence of a lipid bilayer in the system. These non-ionic surfactant containing vesicles are named as niosomes and have been studied for their application in drug delivery. In the following sections, the formulation, preparation and applications of niosomes are discussed and summarized

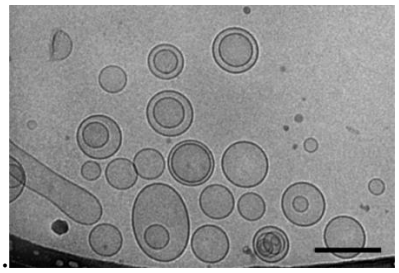

Figure 1-1 Cryo-TEM images of SUVs composed of palmitic acid/cholesterol 30/70 in a pH 9 buffer. Scale bar = 100 nm [5].

1.2 Composition of niosomes

Non-ionic surfactant and cholesterol are two main gradients to construct niosome formulation. Those components determine the mechanisms of the vehicle's formation and their biopharmaceutical fate *in vivo*.

1.2.1 Surfactant

Different types of non-ionic surfactants have been utilized in niosomal vehicle [7]. Tween, Span and Brij were three most commonly used surfactants in niosome[8] [9] [10].(Fig 1-2) Two parameters are considered for the optimal surfactant candidate, including hydrophilic-lipophilic balance (HLB) and critical packing parameter (CPP).

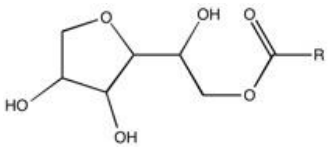

Span

Brij

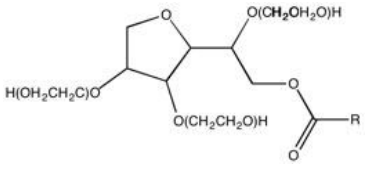

Tween

Figure 1-2 Structure of main surfactant used for niosome

HLB is a parameter to describe the degree of hydrophilicity or lipophilicity of a surfactant. On a scale from 0 to 20, larger the HLB, more water soluble the surfactant is. Surfactants with a HLB number between 3 and 8 are able to form niosome by themselves [7]. Surfactants with higher HLB can also form a bilayer structure with the help of other materials by neutralizing the strong hydrophilicity.

Critical packing parameter predicts the molecular self-assembly in surfactant solution. [11] It is defined by the equation below

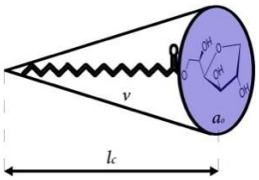

Figure 1-3 CPP definition[7]

Eq.1 $CPP=v/ l_c a_0$

Eq.1, where v, l_c and a_0 refer to hydrophobic group volume, critical hydrophobic group length and the area of the hydrophilic head group, respectively. (Fig.1-2). CPP can predict the general size and shape of the surfactant. The bilayer niosome can only form when this parameter ranges from 0.5 to 1, beyond which the head groups of the surfactants are neither too big nor small. Only in this circumstance can each surfactant molecules occupy a rectangular geometry instead of a conical shape, which is the cornerstone of the bilayer structure.

HLB and CPP were both regarded as important tools for surfactant screening in niosomal formulation. They can depict the mechanism of how vehicle self-assembled. But, up to now, the estimation of these parameters is regarded as hypothetical rather than empirical which can be only used in the single component niosome most of the time[12].

1.2.2 Cholesterol and other helper lipid

Cholesterol is another vital component of niosome. By introducing a hydrophobic group into niosomal membrane system, cholesterol enlarges the repertoire of surfactant candidate. It can affect niosome's critical pharmaceutical parameters including morphology, encapsulation efficiency, stability and i*n vivo* behavior.

Cholesterol can react with surfactant molecules through hydrogen bonding[13]. After inserted into niosomes, cholesterol is able to influence transition temperature of their lipid membrane. In a previous study, 30% cholesterol (molar ratio) in a cholesterol/Span system was sufficient to impart a residual gel/liquid transition enthalpy, a property known as thermo-responsiveness [14], whereas 50 % cholesterol was capable of abolishing gel/liquid transition of the bilayer membranes, resulting in the loss of thermo-responsiveness[15]. High ratio of cholesterol enhanced vehicle's transition temperature and made it stay in gel form at high temperature. Another parameter affected by cholesterol is encapsulation efficiency (EE%). A span 20 based formulation has been reported that the increasing in cholesterol ratio lowered EE% of timolol maleate from 45 ± 2.3 to 30 ± 1.5%. Meanwhile, similar trends were also observed in Span 20 and Span 40 formulations. However, some contradictory evidences were also reported that increasing cholesterol ratio can improve the EE% for a Span 85 based formulation. [16] The mechanisms of how cholesterol can affect encapsulation efficiency have not been elucidated yet. It is determined by the surfactant species and the concentration of cholesterol. One consent among researches is that 50% molar ratio of cholesterol is the optimal cholesterol percentage which can formulate stable niosome with high EE%.[17]

Instead of cholesterol, other lipids are also used as helper lipid with multiple functional purposes in niosomes. Cationic lipid is another helper lipid for niosomes used for gene delivery. Cationic lipid like *N*-[1-(2,3-dioleoyloxy)propyl]-*N*,*N*,*N*-trimethylammonium chloride (DOTAM) can interact with negatively charged DNA or RNA [18], leading to the formation of a niosome-DNA or niosome RNA complex. Solulan C was used as a substitution of cholesterol and stabilized niosomes from aggregation[19]. Dicetyl phosphate is another prevalent additive used to impart a negative charge on the niosomal surface to stabilize its bilayers[20]. Helper lipids can also change endocytosis pathway of niosome. Ediberto Ojeda et al. [21] have made a Tween 80 niosomes incorporated with squalene. Compared with Tween 80/cholesterol niosomes, niosomes with squalene indicated a 4-fold higher transfection efficiency to ARPE-19 cell (31%), due to lysosomal escape effect induced by squalene. Also, Mohamed Mashal et al,[18] have shown that the incorporation of lycopene to the Tween 60 niosome can not only enlarge niosomes' size from 66.49±1.17nm to 101.60±2.48nm, but also induce a higher transfection efficiency which is 10 times higher than the one without lycopene, potentially due to a pinocytosis and raft-mediated pathway of cellular uptake.

1.3 Application of niosome

Reported in 1979, the first niosomal formulation was first applied in cosmetic industry for transdermal delivery[22]. The therapeutic potential of this formulation has attracted great attentions and have been utilized in drug delivery for multiple purposes.

1.3.1 Transdermal delivery

Niosomal formulations have been widely used in transdermal therapy. Topical anti-inflammation therapy is one of the main applications for niosomal formulation.

Celecoxib (CXB) is a nonsteroidal anti-inflammatory drug (NSAID), which exhibits potent anti-inflammatory and analgesic action by inhibiting prostaglandin synthesis by specifically inhibiting the cyclooxygenase-2 (COX-2) enzyme. A Span 60 niosomal polyxamer gel indicated great potential for CXB delivery, allowing a high skin flux in rat model compared with free drug and other gel formulation.[23] Gagan Goyal et al. [24] indicated a benzoyl peroxide loaded niosomal gel formulation. It can increase the inhibition percentage of benzoyl proxide to 41.6% compare with plain drug solution (29.3%) in vitro and also indicate more anti-inflamatory efficacy in vivo based on histological study.

Niosomal formulation can be also used for hypertension therapy. A lacidipine-loaded niosome was reported by Sara Soliman and others. [25] Span 60 and cholesterol were mixed at 2:1 molar ratio to form niosome. *In vivo* study indicated that after 24 hours the niosomal formulation can decrease blood pressure to 118.7 ± 3.9 mmHg compared with the non-treated hypertension rat model 189.5 ± 8.1 mmHg.

1.3.2 Ocular delivery

Niosomes are also applied in ocular delivery. Niosome with size 1.33 ± 0.32 μm was used as vehicle for tacrolimus, an immunosuppresive agent used to treat the intractable allergic conjunctivitis and refractory inflammatory ocular surface diseases. The results showed practical anti-allograft

rejection efficacy *in vivo* on corneal transplantation rats of this formulation. [26] Hyaluronic is a linear polymer composed of long chains of repeating disaccharide units of *N*-acetyl glucosamine and glucuronic acid. Hyaluronic acid can facilitate ocular contact time of the formulation and drug bioavalibility[27]. After coating on the surface of niosome with hyaluronic acid, the ophthalmic bioavalibility was improved by a factor of 1.2 compared with uncoated niosomes. Other drugs like prednisolone[28], lomefloxacin HCl [29] were also used as model drugs to evaluate the potential application of niosome for ocular delivery.

Niosome was also used for gene delivery by intravitreal and subretinal administration. A DOTMA/Tween 60 formulation not only can increase *in vitro* transfection efficiency but also was able to transfect the outer segment of the retina[18]. This offered a reasonable hope for many inherited retinal diseases.

1.3.3 Tumor delivery

Niosomes are also proposed for anti-tumor therapy. The rationale of this application is based on two characteristics of niosomes, stability and adjustable size. The high stability of niosome was considered as the crucial characteristics for its utilization as a long circulating formulation. The high ratio of hydrophilic surfactant on its surface prevents the binding of serum protein which leads to reduced clearance. For some niosomes, the size can be regulated to smaller than 200 nm by different method which make it possible to utilize the enhanced permeation and retention (EPR) effect. EPR effect is based on the fact that blood vessels in tumor areas have large gaps between epithelia cells which allow large vehicles with size smaller than 200 nm reach tumor cells[30]. Meanwhile, the

inefficient lymph system can't drain out those vehicles from tumor tissue, resulting in accumulation of drug in tumor. Due to their small size niosome has great potential for tumor targeting based on EPR effect.

Niosome composed of Span 60, cholesterol and choleth-24 can encapsulate doxorubicin (DOX), an anthracycline anti-tumor reagent, in its hydrophilic core utilizing a passive loading strategy. This formulation indicated a longer blood retention time with AUC increased by 6 fold compared with free DOX. Tumor accumulation increased 1.5 fold in this study[31].

1.4 Research hypothesis and aims of thesis

Niosomes could be an attractive system for systemic delivery of drugs if the size can be controlled below 200 nm with narrow size distribution. However, in an attempt to make niosomes (Tween80/cholesterol = 1/1) using the thin-film hydration method, we found it was challenging to disperse the formulation and perform membrane extrusion to obtain niosomes with good quality. This motivated us to perform research to answer the following questions:

1. Can phospholipid-free small unilamellar vesicle (PFSUV) be fabricated using microfluidics?
2. Do the PFSUVs contain a lipid bilayer?
3. Can a drug be actively loaded into the PFSUVs?
4. How do the PFSUVs behave in cell culture and mice relative to an established PEGylated liposomal formulation?

The thesis contains two specific aims:

Aim 1: To develop PFSUVs using microfluidics for active loading of doxorubicin (DOX)

Aim 2: To compare cellular uptake, in vitro potency, pharmacokinetics and biodistribution of DOX-loaded PFSUVs with PEGylated liposomal doxorubicin (PLD)

Chapter 2: Develop phospholipid-free small unilamellar vehicles (PFSUVs) using microfluidics for active loading of doxorubicin (DOX)

2.1 Materials

Tween 80, cholesterol, ammonium sulfate, sheep red blood cells, DOX and HEPES (4-(2-hydroxyethyl)-1-piperazineethanesulfonic acid) were purchase from Sigma-Aldrich (St. Louis, MO). Ultra-pure water was prepared in our laboratory using Milli-Q Synthesis system (Millipore, Merck, Darmstadt, Germany). Free cholesterol E assay kit was purchased from Wako Chemicals USA Inc. (Richmond, VA)

2.2 Methods

2.2.1 Preparation of PFSUVs

PFSUVs with different Tween 80/cholesterol molar ratios (1:1.5, 2:1, 3:1, 5:1, 8:1) were fabricated in a controlled nanoprecipitation process using a two-channel microfluidic system (NanoAssemblr, Precision Nnaosystems International, Vancouver, BC, Canada). Lipids were dissolved in ethanol at a final concentration of 10 mg/ml and were mixed with 120 mM ammonium sulfate (AS) solution in the NanoAssemblr at a flow ratio of 1/3. The total flow rate is 15 ml /min. The mixture was then dialyzed (slide-A-Lyzer, 10000 MWCO) against HEPES buffered saline (HBS, pH 7.4) for 12 h, with fresh HBS replaced at 2 h and 4 h. Cholesterol concentration in PFSUVs after dialysis was determined by a cholesterol E assay kit. Particle size was measured using a particle analyzer (Zetasizer NanoZS, Malvern Instruments Ltd. Malven, UK).

2.2.2 Short term storage stability of empty PFSUVs

Empty PFSUVs with different Tween 80/Cholesterol ratios were stored at 4 ℃ in a glass vial. At selected time points, the size of each sample was measured as described before.

2.2.3 DOX loading

PFSUVs (1.5 mg total lipids) were incubated with 100 µg DOX in a total volume of 1 ml. The mixture was incubated for 1 h at 20 ℃, 37 ℃, 45 ℃ and 60 ℃, respectively and then quenched on ice for 2 min. Encapsulation efficiency(EE%) was calculated following a UV/Vis spectroscopy method described in an earlier publication with some modifications [32]. The method utilized the property of DOX whose maximum absorbance undertakes a red-shift from 480 nm to 600 nm when the pH increases to 14. Adding NaOH to PFSUVs increased the pH of the exterior buffer to 14 and the unencapsulated DOX revealed a maximum absorbance at 600 nm, while the loaded DOX exhibited little absorbance at 600 nm. Briefly, 10 µl of PFSUVs-Dox was mixed with 2 µl NaOH (4 M) and 2 µl HBS, and was then transferred immediately to a Thermoscientific NanoDrop 2000 spectrophotometer to detect the absorbance at 600 nm. The final encapsulation efficiency was calculated by the following equation.

Eq.2 $EE\% = 1 - \frac{Rs-R0}{R100-R0}$

Where Rs is the absorbance of the sample. R0 is the absorbance of mixture containing 10 µl PFSUVs-DOX and 4 µl HBS. R100 is the absorbance of 10 µl PFSUV-DOX mixed with 2 µl NaOH (4M) and 2 µl Triton-X 100 (10%).

2.2.4 Loading kinetic

DOX (100 µg) was incubated with PFSUVs (1.5 mg total lipids) for 5, 15, 30 or 60 min at 20 ℃, 37 ℃ or 60 ℃. The mixture was quenched in an ice bath for 2 min to terminate the loading procedure. EE% was measured using the method described earlier.

2.2.5 Effect of drug/lipid ratio

DOX and PFSUVs were mixed at different drug/lipid ratios (from 1:5 to 1:25) at 37 ℃ for 1h, and the encapsulation efficiency was measured by the previous method.

2.2.6 Hemolysis study

Forty µl sheep red blood cells (SRBC) were mixed with different amounts of PFSUVs-DOX in a 96-well plate (Greiner bio-one, Germany), incubated at 37 ℃ for 30 min and centrifuged at 5000g for 10 min at 4°C. The supernatant was collected and measured for the absorbance at 540 nm using a microplate reader (Hidex Sense, Hidex, Finland). PBS and Triton-X 100 (10%) were used as the negative control and positive control, respectively. Relative hemolysis (RH) of PFSUVs was calculated using the equation below:

Eq.3 $RH\% = \frac{Rs - Rn}{Rp - Rn}$

Where Rs, Rn and Rp are the absorbance readings of PFSUVs-DOX, negative control and positive control respectively.

2.2.7 Cryo-transmission electron microscopy (cryo-TEM)

The morphology of the empty PFSUVs and PFSUVs-DOX was imaged by a FEI Tecnai G20 Lab6 200 kV TEM (FEI, Hillsboro, OR) following a previously described method[33]. The instrument was operated at 200 kV in bright-field mode. Digital images were recorded under low dose conditions with a high-resolution FEI Eagle 4 k CCD camera (FEI, Hillsboro, OR) and analysis software FEI TIA. A nominal under focus of 2-4 μm was used to enhance image contrast. Sample preparation was performed using the FEI Mark IV Vitrobot. Approximately 2-4 μl of PFSUVs at ~20 mg lipid /mL was applied to a copper grid and plunge-frozen in liquid ethane to generate vitreous ice. The frozen samples were then stored in liquid nitrogen until imaged. All samples were frozen and imaged at the UBC Bioimaging Facility (Vancouver, BC).

2.2.8 Statistical analysis

All data are expressed as mean ± SD. Statistical analysis was conducted with the two-tailed unpaired t test for two group comparison or one-way ANOVA, followed by the Turkey multiple comparison test by using GraphPad Prism (for three or more groups). A difference with $p < 0.05$ was considered to be statistically significance.

2.3 Results

2.3.1 Effect of cholesterol/Tween 80 ratio on the size of PFSUVs and the short-term stability

PFSUVs with different cholesterol/tween 80 ratios were formulated by the microfluidics. As indicated in Fig.2-1, the cholesterol/Tween 80 ratio had minimal effect on the size as most

formulations exhibited a mean diameter between 60 and 70 nm. However, when the cholesterol ratio increased to approximately 90%, the particle size increased to 115.0±5.6 nm.

The stability of PFSUVs at 4 °C was monitored by measuring the size over time. All the formulations were stable for 10 days except for the one composed of cholesterol/Tween 80 (8:1), and the size increased from 115.0±5.6 nm to 176.6±21.2 nm. No visible precipitates were spotted in the PFSUV formulations after 10 days of storage. We concluded that the 8:2 formulation was not suitable for drug delivery.

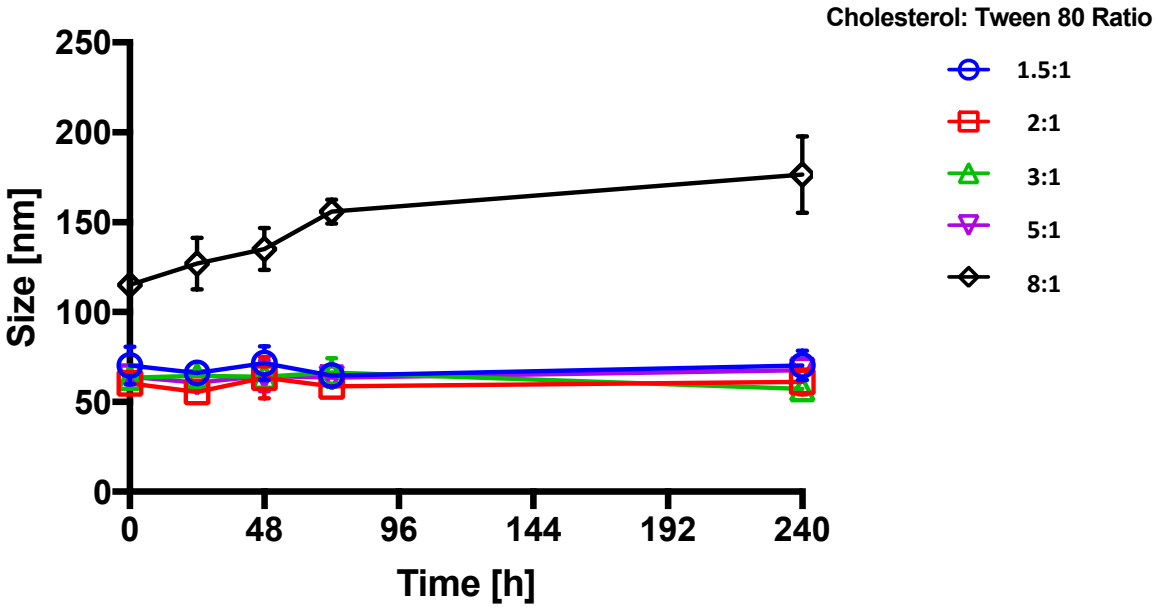

Figure 2-1 Stability of empty PFSUVs stored at 4°C. Data = mean ± SD (n=3)

2.3.2 Optimization of DOX loading

We then investigated whether DOX could be actively loaded into different PFSUV formulations and whether the incubation temperature affected the encapsulation efficiency and the particle stability. As shown in Fig 2-2 (A), when loading at 37°C or below, there was no change in size of the final particles. However, when the incubation temperature increased to 45°C, the high Tween80 formulation (1.5:1) displayed a significant increase in size to ~150 nm. When the loading temperature further increased to 60°C, the particle size increased in all the formulations (100-170 nm). The EE% was also impacted by the lipid formulation and loading temperature. As shown in Fig.2-2(B), only formulations containing a lower amount of Tween80 (3:1 and 5:1) could load DOX via an active mechanism. For the 3:1 formulation, the EE% at 20-45°C was comparable (~80%), while there was no drug loading at 60°C. On the other hand, the drug encapsulation efficiency for the 5:1 formulation displayed an increasing trend (from 70% to 90%) with increasing temperature (from 25°C to 45°C), except that at 60°C the EE% declined back to 70%.

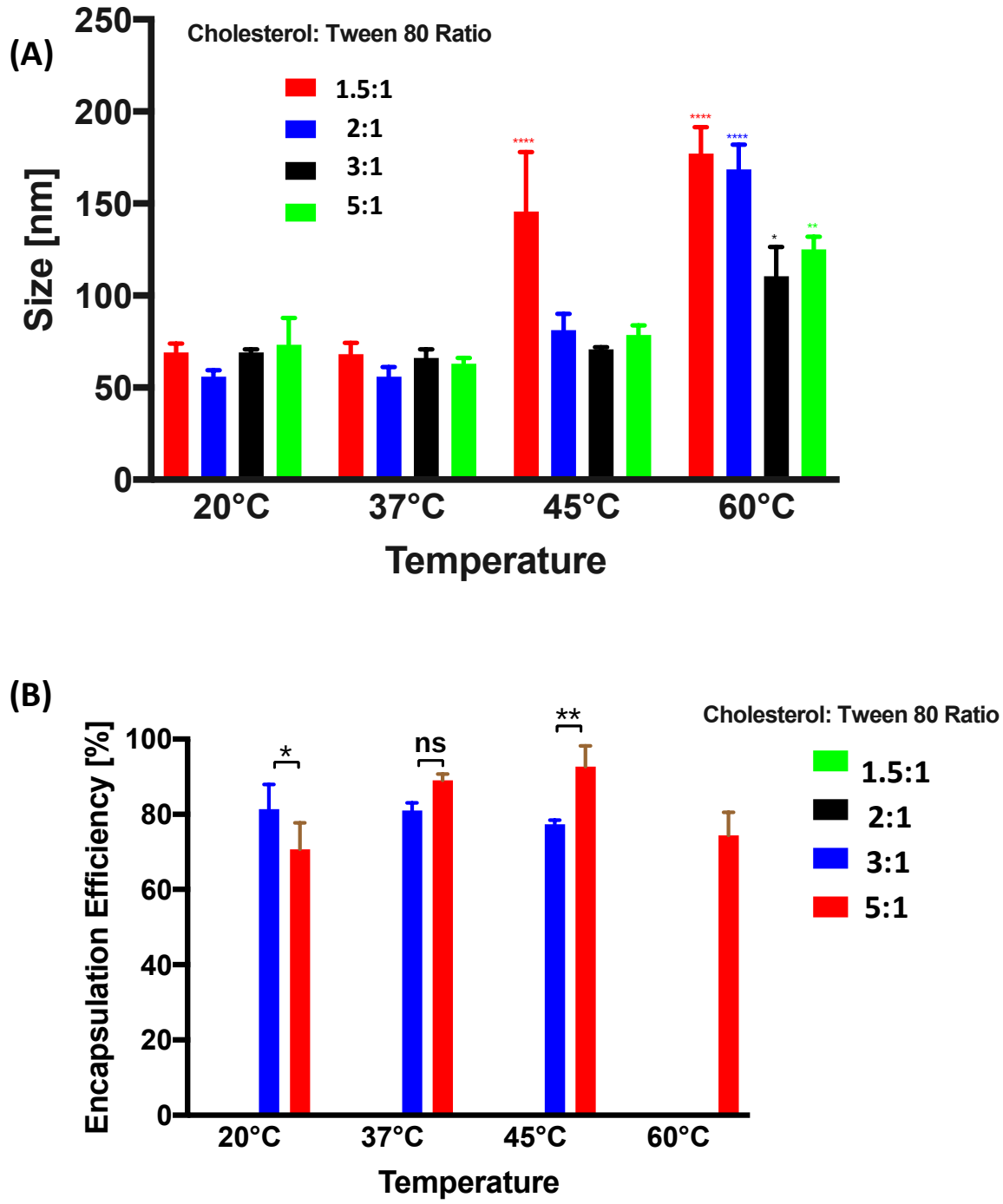

Figure 2-2 The impact of loading temperature and lipid composition on the size (A) and drug encapsulation efficiency (B). Data = mean ± SD (n=3). *: P<0.05; **: P<0.002; ***: P<0.0002; ****: P<0.0001

2.3.3 Loading kinetics

DOX EE% at different time points under different incubation temperature was measured. As shown in Fg.2-3, the drug loading kinetics was dependent on the loading temperature and incubation time. As the incubation temperature increased, the drug EE% increased and reached the maximum faster. For example, at 20°C, the EE% slowly reached the maximum at ~60% after 30-60 min of incubation, while the loading reached the plateau of ~90% in 15 min when incubated at 45°C. At 37°C, it took 30-60 min to achieve ~90% of drug loading.

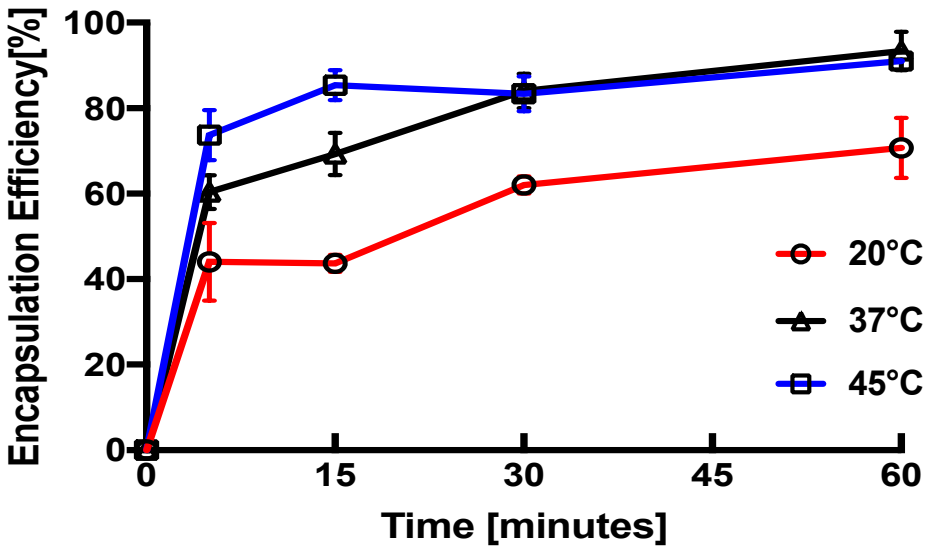

Figure 2-3 DOX loading kinetics into PFSUVs at different temperatures. Data = mean ± SD (n=3).

2.3.4 Drug /Lipid ratio

To investigate the loading capacity of the PFSUVs, drug EE% at different drug-to-lipid ratio (D/L) was compared. As shown in Fig 2-4., drug EE% gradually decreased as D/L increased, and the highest D/L was 1/20 for complete drug loading (>95%).

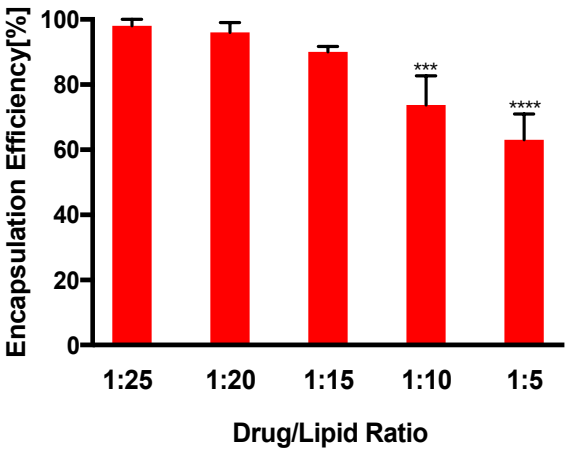

Figure 2-4 Drug EE% of PFSUVs with different drug/lipid ratios. Data = mean ± SD (n=3). *: P<0.05; **: P<0.002; ***: P<0.0002; ****: P<0.0001

2.3.5 Hemolysis

Hemolytic toxicity of the PFSUVs-DOX was measured by incubating the formulation at different concentrations with SRBC. The concentrations labeled in Fig.2-5 indicated the final DOX concentration, and the PFSUVs exhibited little hemolytic toxicity.

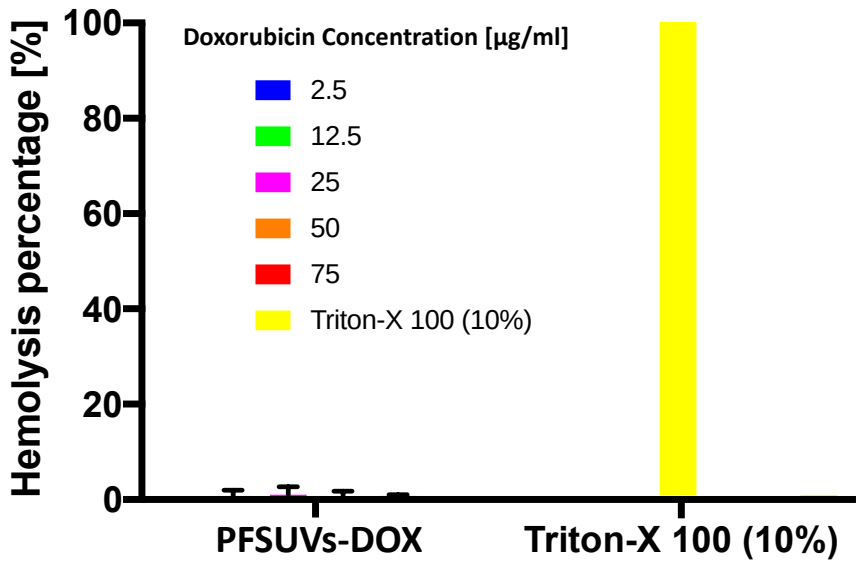

Figure 2-5 Hemolytic toxicity of PFSUVs-DOX at different concentration. Data = mean ± SD (n=3)

2.3.6 Cryo-TEM images of PFSUVs

As shown in Fig.2-6, the empty PFSUVs displayed a bilayer structure with a spherical morphology (panel A) and DOX crystalline was found in the aqueous core of the SUVs (panel B). The formation of DOX crystalline inside the PFSUVs did not alter the particle morphology compared to the empty vehicle.

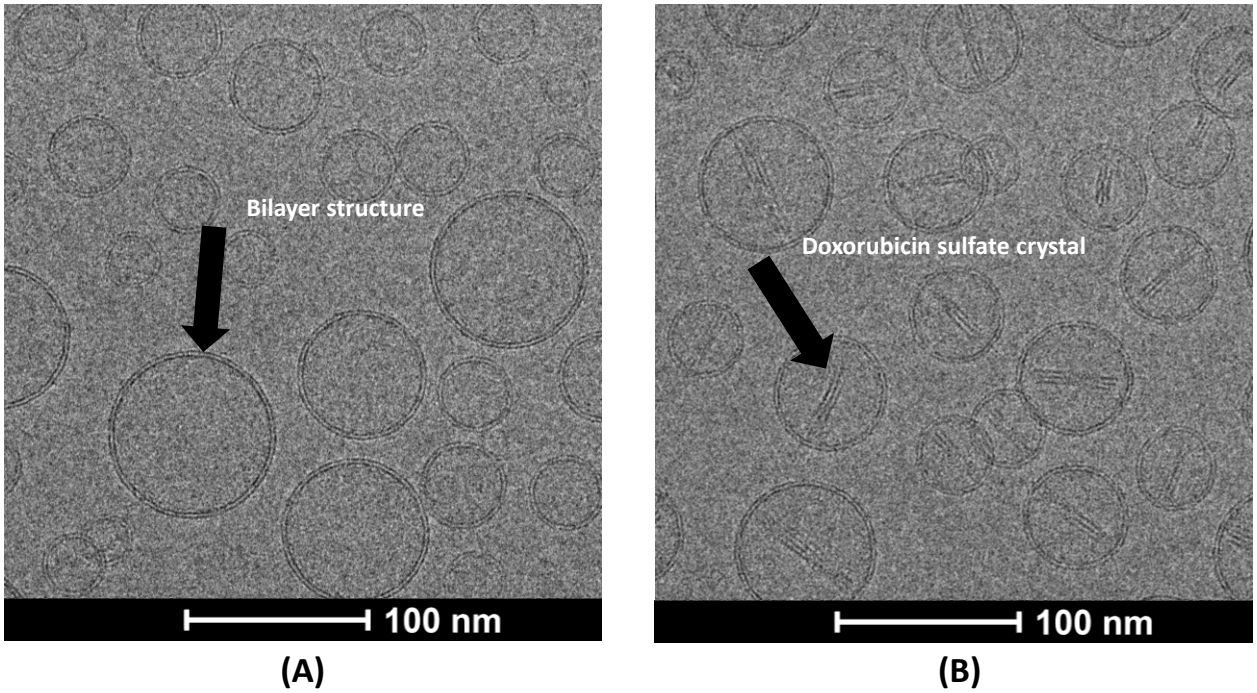

Figure 2-6 Cryo-TEM images of empty PFSUVs (A) and PFSUVs-DOX (B). Arrows indicate bilayer (A) and DOX crystalline (B), respectively.

2.4 Discussion

We successfully fabricated stable PFSUVs with a small diameter (60-80 nm) under a cholesterol/Tween 80 ratio ranging between 1.5:1 and 5:1 by a microfluidic method. When the cholesterol content increased to 90%, formulation exhibited a larger size (~150 nm) and the size grew over time during 4°C storage. This could be due to precipitation of cholesterol in the bilayer when the content exceeded 80% of the bilayer composition. It was previously demonstrated that niosomes prepared with the thin-film hydration method were not stable when the cholesterol content reached 80%[37, 38].Therefore, in most reports, niosomes were prepared at 5:5 ratio between cholesterol and a non-ionic surfactant. The data suggest that the preparation method could affect the formation of

phospholipid-free bilayer, influencing the product stability. During the microfluidic process, rapid mixing of the ethanol/lipid solution with the aqueous phase resulted in a rapid increase in the polarity of the medium, which caused the solution to quickly achieve a state of high supersaturation of lipid monomers throughout the entire mixing volume,[39] leading to rapid and homogeneous nucleation of lipid bilayer. These nucleation events were very rapid (< 1 ms) compared to the time-scale for particles' formation[39]. Therefore, it is suggested that by using microfluidics, cholesterol could be dispersed in the bilayer more rapidly and efficiently, leading to improved stability.

We then explored potential application of this phospholipid-free system to deliver a drug. Hydrophilic and hydrophobic drugs can be dissolved in the aqueous phase and with the lipids to be passively loaded into the inner aqueous core and the lipid bilayer, respectively. Active loading, on the other hand, utilizes a cross membrane gradient to for encapsulating drug 'remotely' inside the liposomal core, resulting in increased encapsulation efficiency and improved drug retention. For example, to load doxorubicin (DOX, a weak base drug, Fig. 2-7), an ammonium sulfate gradient is created cross liposomes (inner core: 250 mM ammonium sulfate, pH 5; outer phase: HEPES buffered saline, pH 7.4). DOX is dissolved in the outer phase and incubated with the preformed liposomes at 65˚C for 1 h. This high temperature incubation significantly increases the lipid membrane permeability,resulting in the permeation of non-ionized form Dox into the liposomal Under this acidic environment in liposome, DOX is protonated and no longer membrane permeable. The protonated DOX can form complexes with the sulfate ion inside the core, generating insoluble precipitates inside the liposomes. This irreversible process drives effective loading and DOX precipitation inside the liposomal core leading to reduced drug leakage. Active DOX loading into niosomes has never been

reported before. It was believed that this phospholipid-free bilayer (mainly cholesterol/surfactant 5:5 formulation) was not stable enough to hold the loading gradient. As we obtained PFSUVs with a range of cholesterol/Tween ratio, we tested their ability to maintain a loading gradient of 120 mM ammonium sulfate. Indeed, when the Tween80 content was above 35%, no DOX loading was measured under all the tested conditions, while >80% DOX could be actively loaded into PFSUVs containing 25% and 17% Tween80 when incubated at 20-45°C. Interestingly, when incubated at 60°C, no DOX loading into the 3:1 formulation was measured, while 75% loading efficiency was obtained within the 5:1 formulation, suggesting heating could disrupt the membrane integrity for a formulation containing an increased amount of surfactant. Therefore, our data indicate the optimal PFSUVs formulation was 5:1 cholesterol:Tween80, which exhibited a small (60-80 nm) and stable particle size. The formulation is capable to maintain a loading gradient for active encapsulation of DOX under a wide range of conditions. Finally, the loading kinetics of the PFSUVs followed a similar pattern as the regular liposomes, for which as the incubation temperature increased the rate and amount of drug loading increased.

To the best of our knowledge, this was the first work with cryo-TEM images showing SUVs containing a phospholipid-free bilayer with DOX crystalline loaded inside the aqueous core. The bilayer structure of niosomes was suggested mainly based on the data that niosomes could encapsulate highly water soluble compounds, but there has not been any visual proof of a phospholipid-free bilayer

The images provided direct proofs that cholesterol: Tween80 (5:1) formed a bilayer structure that could maintain a gradient for active loading of DOX. Interestingly, the PFSUVs remained their

spherical shape after DOX loading, while PLD displayed an oval morphology due to the big size DOX crystalline inside the liposomes. This can be explained by that the D/L in the PFSUVs was only ~1/3 of that in the PLD, and the small size of DOX crystalline did not alter the SUV shape.

In summary, we have fabricated PFSUVs containing cholesterol and Tween80, and the 7:3 formulation was demonstrated to be optimal for active loading of DOX. Preparation parameters including formulation and loading conditions were optimized to produce stable and small size PFSUVs that provided complete loading of DOX at a D/L of 1/20. The formation of this DOX loaded, bilayered PFSUVs were evidenced with cryo-TEM images.

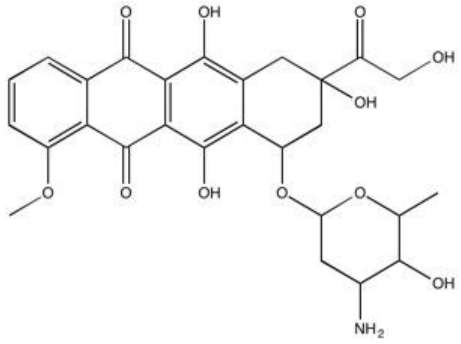

Figure 2-7 Structure of Dox

Chapter 3: compare cellular uptake, in vitro potency, pharmacokinetics and biodistribution of DOX-loaded PFSUVs with pegylated liposomal doxorubicin (PLD)

3.1 Materials

3.1.1 Reagents

1,2-Disteary-sn-glycero-3-phospatidylcholine (DSPC) and 1,2-disteroyl-sn-glycero-phosphatiylethanol-amine-N-[methoxy (polyethyleneglycol)-2000] (DSPE-PEG2000) were purchased from Avanti Polar Lipids (Alabaster, AL). Thiazolyl Blue tetrazolium bromide was purchased from Alfa Aesar (Tewksbury, MA). Fluoroshield with DAPI was purchased from Sigma (Laramine, WY).

3.1.2 Cancer cell line

EMT6 (murine breast cancer) cells were purchased from National Cancer Institute (Bethesda, MD).

3.1.3 Mice

Female BALB/c mice (6-8 weeks old) were purchased from the Jackson Laboratory (Bar Harbor, ME). The experimental protocol has been approved by the Animal Care Committee of University of British Columbia.

3.2 Methods

3.2.1 Preparation of PLD and its characterization

The thin-film hydration method was utilized to prepare PLD as described before with some modifications.[36] Briefly, 32 mg of lipid (DSPC/Chol/DSPE-PEG2000 = 38/25/4, molar ratio) was dissolved in chloroform. The organic solvent was then removed by rotary evaporation (BUCHI, Flawil Switzerland) at 60 °C. The thin film was hydrated with 250 mM ammonium sulfate at 60 °C for 45 min and then sonicated for 10 min with a water-bath ultrasound. The lipid suspension was extruded through 100 nm and 50 nm Nuclepore Track-Etch Membrane (Sigma, Laramine, WY) for 10 times successively using a mini extruder (Avanti Polar Lipids, Inc, Alabaster, AL). Liposomes were dialyzed (1: 1000, volume ratio) against HEPES-buffered saline (HBS, pH 7.4) overnight afterwards. The final lipid concentration of liposomes was determined by a cholesterol assay kit.

One mg DOX was mixed with 8 mg (total lipid) empty liposomes at a total volume of 1 ml adjusted by HBS. The loading mixture was incubated at 60 °C for 45 min and then quenched on ice for another 2 min. Free DOX was then removed by dialysis (1: 1000, volume ratio) against HBS for 8 h. PLD was subsequently filtered through 0.22 μm membrane for sterilization. The final concentration of DOX in PLD was measured by the fluorescence (excitation: 485 nm; emission: 590 nm) and compared with a standard curve. PLD was characterized for its size, polydispersity index (PDI), and zeta potential by a Zetasizer. The DOX encapsulation efficiency was measured following the method described in Chapter 2.

3.2.2 Preparation of PFSUVs-DOX (Fig. 3.1.)

PFSUVs dispersed in 120 mM ammonium sulfate were produced by the NanoAssemblr Benchtop described in Chapter 1. Fifty ml of the PFSUVs were subjected to a tangential flow filtration system (TFF) (Ki2, Kroso TFF system, Spectrum Labs, Canada) to remove ethanol, exchange the exterior phase to HBS and concentrate. In the TFF system, the PFSUVs flew through a diafiltration cartridge with a molecular weight cut-off of 50 kD (Midikros, hollow fiber filter module, spectrum Labs, Canada) at a flow rate 140 ml/min. The PFSUVs were concentrated to 30 mg/ml.

One mg DOX and 20 mg (total lipid) PFSUVs were mixed in a final volume of 1 ml HBS. After incubated at 37 °C for 1 h, PFSUVs-DOX was quenched on ice for 2 min. The rest of the procedures were the same as reported in section 3.2.1.

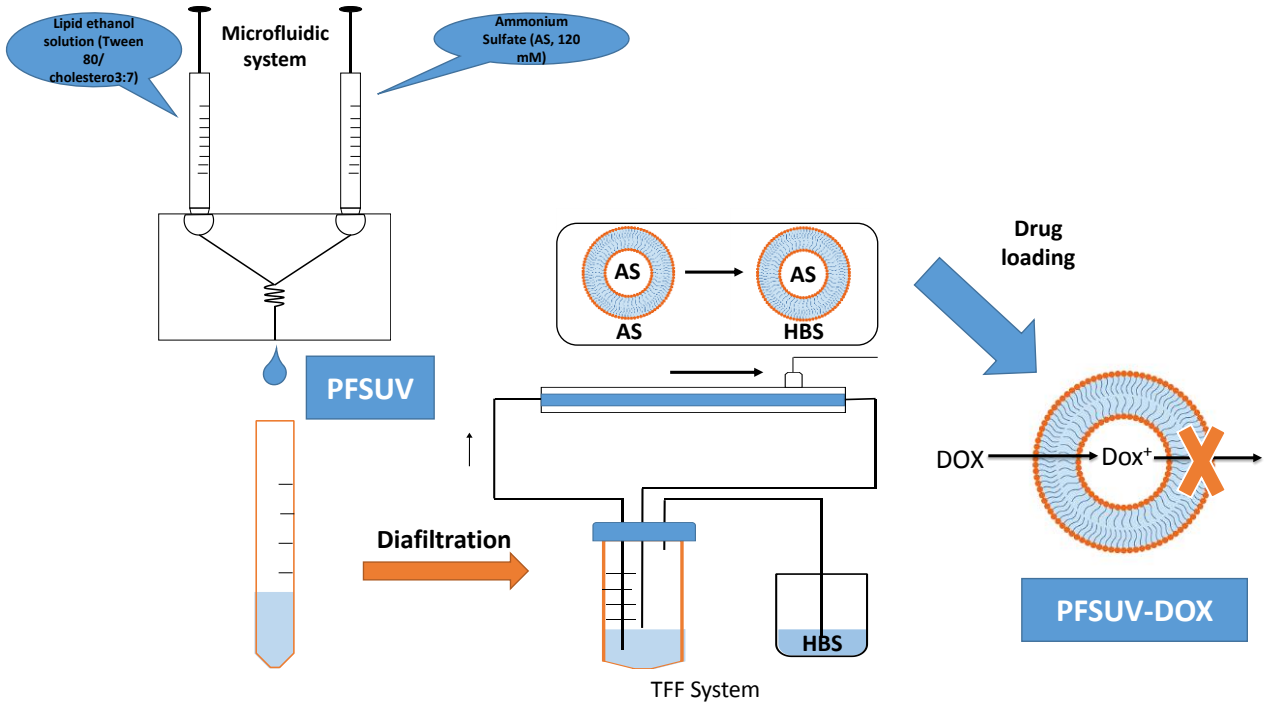

Figure 3-1 Preparation method for PFSUVs-DOX

3.2.3 In vitro drug retention

PLD and PFSUVs-DOX were adjusted their DOX concentration to 50 μg/ml by sterile PBS, mixed with 1:1 sterile FBS, and then incubated at 37 °C. At selected timepoints, 10 μl of the sample was collected and diluted with PBS for 30-fold. The diluted sample was transferred to a 96-well plate (225 μl sample + 25 μl PBS) for fluorescence detection using a microplate reader (Ex 485 nm/Em 595 nm). The percentage of drug retention at each time point was calculated as [1-(Ft-F0)/(Ft-F100)]×100%, in which Ft is the fluorescence at each selected time point, F0 is the fluorescence at time 0 and F100 is the fluorescence of the sample prepared by mixing 225 μl diluted sample and 25 μl Triton-X 100 (10%), followed by incubation at room temperature for 15 min in dark.

3.2.4 Cell culture

EMT6 cells were cultured in DMEM medium with 10 % FBS, penicillin (100U/ml) and streptomycin (100 μg/ml) at 37 C with 5% CO2.

3.2.5 In vitro cytotoxicity

EMT6 cells were seeded on a 96-well plate (1000 cells/well). Wells with medium only were used as blank. After 24 h of incubation, cells were treated with different concentrations of free DOX, PFSUVs-DOX and PLD. Two days later, 5 μl of MTT solution (5 mg/ml) was added to each well, followed by 4-h incubation. The medium was removed and 100 μl DMSO was added into each well, followed by incubation at room temperature for 15 min. Absorbance at 540 nm in each well was

then measured by a plate reader. The cell viability was calculated as $(Ab_s-Ab_{blank})/(Ab_{100}-Ab_{blank})\times100\%$, where Ab_s is the $Absorbance_{540nm}$ for the experimental group, Ab_{blank} is the $Absorbance_{540nm}$ of sample without cells and Ab_{100} is the $Absorbance_{540nm}$ of sample without treatment.

3.2.6 Cellular uptake

Cellular uptake of DOX was imaged by confocal laser scanning microscopy (CLSM). EMT6 cells were seeded on a cover slip placed in a 24-well plate (1×10^5 cell/well) for 24 h prior to the study. Cells were treated with DOX, PLD or PFSUVs-DOX at a concentration 5 μg DOX/ml in the presence or absence of 10% FBS for 4 h. The medium was removed and the cells were washed with PBS twice before fixation with 10% of formaldehyde at room temperature for 20 min. The cover slip was then washed for another 2 times with PBS and mount on a glass slide with fluorescence shield containing DAPI. The cells were imaged under a Zeiss confocal microscope (LSM 700) and the image was analyzed using the CellProfiler (Version 3.0) software.

3.2.7 Subcutaneous EMT6 tumor model

Approximately 1×10^5 EMT6 cells were subcutaneously injected to right flank of BALB/C mice. Mice were subjected for in vivo studies when the tumor reached a volume of ~200 mm^3.

3.2.8 Pharmacokinetics

PLD and PFSUV-DOX (5 mg DOX/kg) were administered to tumor-bearing mice via tail vein injection. Mice were euthanized at various time points. About 100 μl blood was collected from mice by cardiac puncture. Plasma was immediately isolated by centrifugation of the blood at 4 °C for 15 min at 2,500 rmp. The plasma concentration of DOX was measured by a previously reported method[37]. Briefly, 10 μl of plasma was diluted with 990 μl acidified isopropanol (IPA) and the mixture was incubated at 4 °C in the dark for overnight. The sample was then centrifuged for 10 min at 12,000 ×g and the supernatant was loaded onto a 96-well plate for fluorescence determination (Ex 485 nm/Em 595 nm). The plasma concentration was then obtained by comparing the fluorescence with a calibration curve generated by spiking known amounts of DOX into mouse plasma.

3.2.9 Biodistribution

After the euthanasia of the mice, different tissues including heart, liver, spleen, kidney, lung, tumor and brain, were excised. The experimental procedures were adapted from the previously published literature[37]. The tissue was washed with PBS, weighed after removing excess fluid and put into a 1.5-ml microtube. Normally, 0.1–0.3 g tissue was collected. The nuclear lysis buffer (10 mM HEPES, 1 mM MgSO4, 1 mM CaCl2, pH 7.4) with a volume three times to the tissue weight was added into the microtube, and tissue homogenization was performed for 2 × 30 s at 6,600 rpm with a tissue homogenizer (Precellys 24, Bertin Technologies, Cartland, CA). An aliquot of the homogenate (100 μl) was transferred into a 1.5 ml microtube, and 50 μl of 10% (v/v) Triton X-100, 100 μl of water, and 750 μl of acidified IPA were added and the mixture was stored for overnight at −20 °C. The

mixture was then thawed, equilibrated at room temperature for 1 h, centrifuged for 10 min at 12,000×g, and the supernatant was loaded onto a 96-well plate (Ex 485 nm/Em 590 nm) for DOX determination. The data was compared with standard curves made from spiking known amounts of DOX into different tissue homogenates from the untreated mice to get the absolute quantification of DOX in different tissues.

3.2.10 Tissue section

Liver in the PFSUVs-DOX treated mice was harvested 2 h post injection, fixed in 10 % formaldehyde, sectioned using a vibratome (Precisionary Instruments, Boston, MA). Tissue sections with a thickness of 40 μm were collected in PBS and then stained with fluorescien-phalloidin (40U/ml) for 15 min at room temperature. The sections were imaged under confocal microscopy.

3.2.11 Statistics analysis

All data are expressed as mean ± SD. Statistical analysis was conducted with the two-tailed unpaired t test for two group comparison or one-way ANOVA, followed by the Turkey multiple comparison test by using GraphPad Prism (for three or more groups). A difference with $p < 0.05$ was considered to be statistically significant.

3.3 Results

3.3.1 Characterization of PFSUVs-DOX and PLD

Both PLD and PFSUVs-DOX were characterized by the size, PDI, zeta potential (ZP) and EE%. Their formulation parameters are compared in Table3.1. PFSUVs-DOX prepared by microfluidics

were significantly smaller than the PLD fabricated by membrane extrusion. PFSUVs-DOX exhibited neutral surface charge with a ZP close to 0 mV, while the PLD displayed negatively charged surface (-25 mV). The PLD provided an increased D/L compared to PFSUVs-DOX, indicating a higher drug content per particle.

Formulation	Composition	Method	D/L ratio	Size (nm)	PDI	ZP (mV)	EE%
Phospholipid free small Unilamellar Vehicle (PFSUV)	Tween 80/Cholesterol (1/5)	Microfluidic method	1:20	74.67±4.51	0.132±0.027	-5.49±3.68	96±3.2
PEGylated Liposomal Doxorubicin(PLD)	DSPC/DSPE-mPEG2000/Cholesterol (38/4/25)	Thin- film Extrusion method	1:8	111.30±9.67	0.036±0.023	-24.7±1.9	95±1.1

Table 3-1 Comparison between PFSUVs-DOX and PLD.

3.3.2 In vitro drug retention

As shown in Fig.3-2, during the first 3 days of incubation with 50% FBS, no DOX release was detected from neither PFSUVs-DOX or PLD. Six days later, approximately 10% of DOX was released from PFSUVs-DOX, while no drug leakage was measured with PLD.

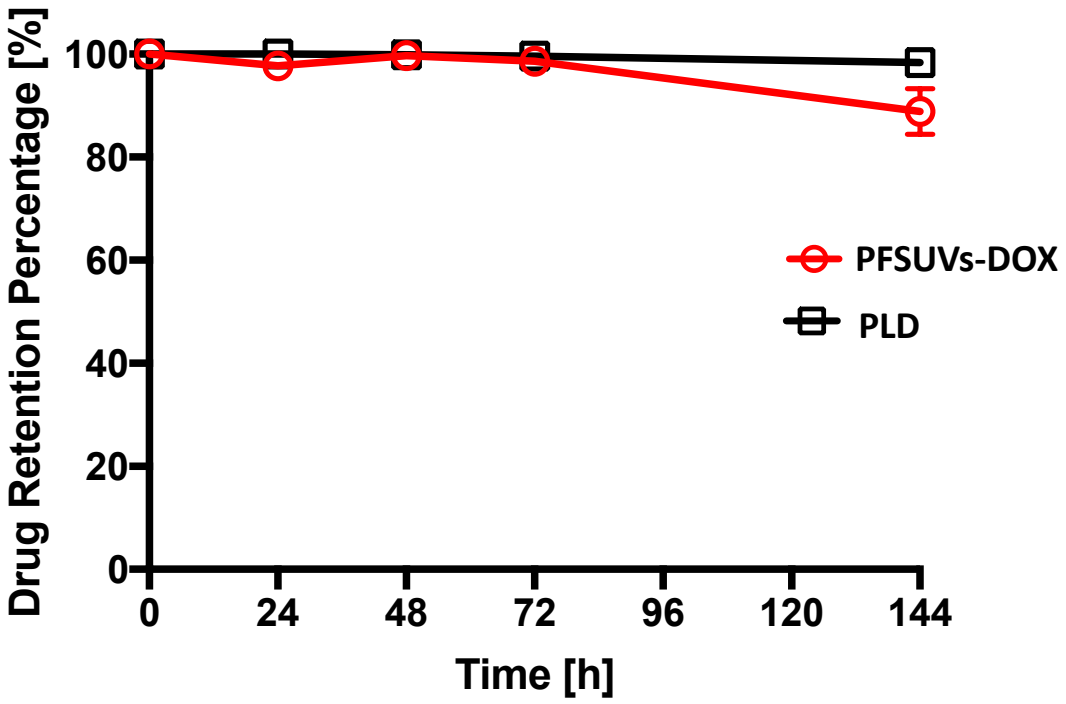

Figure 3-2 in vitro DOX retention in PLD and PFSUVs-DOX in 50% FBS at 37 °C. Data = mean ± SD (n=3)

3.3.3 Cellular Uptake

Intracellular delivery of DOX by different formulations was analyzed by CLMS imaging, and the images were quantified by CellProfiler. As shown in Fig.3.3A, in the absence of serum, DOX uptake in the PFSUVs-DOX and PLD groups was minimal, while free DOX displayed highly efficient co-localization with the nucleus. In the presence of serum (Fig 3.3B), there was a significant increase in DOX uptake in the PFSUVs-DOX group compared to the serum free conditions. The presence of serum did not significantly change the DOX uptake in free DOX and PLD groups. The quantitative data showed that free DOX displayed ~15-fold increased cellular uptake relative to PFSUVs-DOX and PLD in the absence of serum, while the intracellular delivery

of PFSUVs-DOX was increased by 2-fold in the presence of serum. Such effect was not observed in free DOX and PLD groups.

Mean Fluorescence Intensity

	Without Serum	10% Serum
PFSUVs -DOX	0.015±0.002	0.029±0.004
PLD	0.016±0.003	0.015±0.001
DOX	0.258±0.014	0.247±0.021

Table 3-2 Mean fluorescence intensity in each EMT6 cell after 4 h treatment with DOX, PLD and PFLUV-DOX. The results were quantified using cell profiler software based on the result of confocal imaging. (n>30)

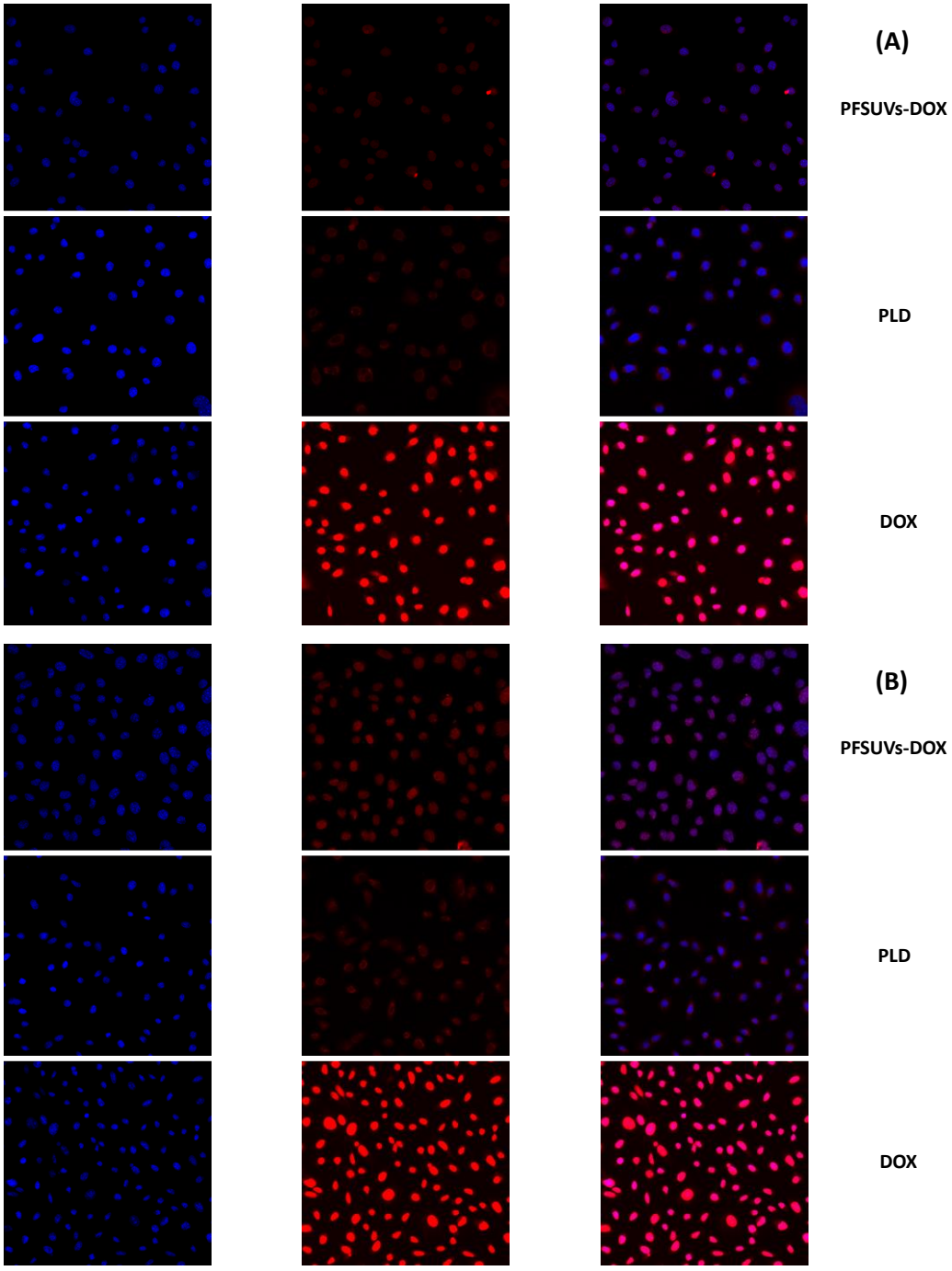

Figure 3-3 Cellular uptake of DOX formulated in different formulations in the absence (A) or presence (B) of 10% FBS. Red = DOX; blue = DAPI, nucleus.

3.3.4 In vitro cytotoxicity

In vitro cytotoxicity of free DOX, PFSUVs-DOX and PLD against EMT6 murine breast cancer cells was evaluated by MTT assay, and the IC50 values were obtained by curve fitting using GraphPad. As shown in Fig 3.4, the curves of free DOX and PFSUVs-DOX were largely overlapping, suggesting comparable potency, while the PLD was significantly less potent in inhibiting EMT6 cells. The IC50 values for free DOX, PFSUVs-DOX and PLD were 25, 94 and 1658 ng/ml, respectively. PLD was 20-fold less effective compared to PFSUVs-DOX for the in vitro potency. And DOX indicated 4-fold more effective than PFSUVs-dox for the in vitro potency.

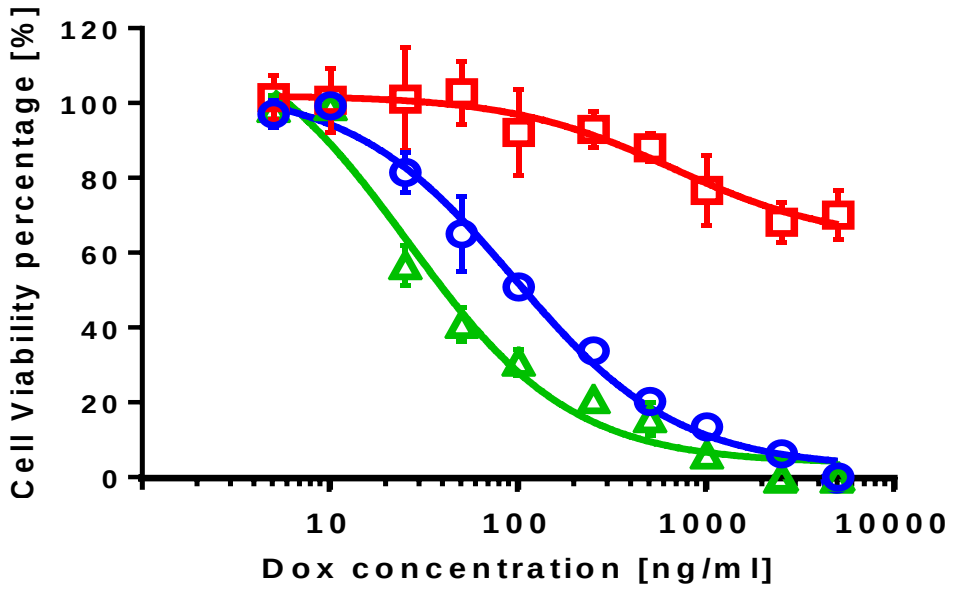

Figure 3-4 EMT6 cell viability after 3-day treatment with free DOX, PFSUVs-DOX and PLD at different DOX concentrations.

3.3.5 Pharmacokinetics

Plasma concentration of DOX was measured at different timepoints after an i.v. injection of PFSUVs-DOX and PLD and was plotted in Fig 3.5. PLD displayed prolonged plasma circulation

profile and the plasma concentration declined slowly from 2 h (183.5 μg/ml) to 48 h (37.2 μg/ml). DOX in the PFSUVs-DOX treated mice could only be detected 2 h post injection (4.7 μg/ml), indicating PFSUVs-DOX were rapidly removed from the plasma.

3.3.6 Biodistribution

DOX concentration in different tissues at different time points after treatment with PFSUVs-DOX or PLD was measured and reported in Fig 3.6. The PLD formulation selectively accumulated in the tumor, liver and spleen (> 1.5 μg/g tissue), and displayed minimal uptake by other tissues, including the brain, lung, kidney and heart (< 0.3 μg/g tissue). The data also showed that there was a gradual increase of PLD uptake in the tumor, liver and spleen from 2-48 h. In 48 h, PLD uptake in these tissues reached the maximum with 1.3 μg/g, 5.7 μg/g and 5.4 μg/g measured in the tumor, liver and spleen, respectively. On the other hand, PFSUVs-DOX showed early uptake (2 h) in tissues, including the tumor, brain, liver and spleen, but the concentration rapidly declined to background in the brain and liver. The tumor uptake of PFSUVs-DOX stayed consistently from 2-48 h at 0.34 μg/g, and the spleen uptake only dropped from 5 μg/g to 2.5 μg/g from 2 h to 48 h. The most significant uptake of PFSUVs-DOX occurred in 2 h in the liver, showing ~15 μg/g, but rapidly decreased to almost undetectable in one day.

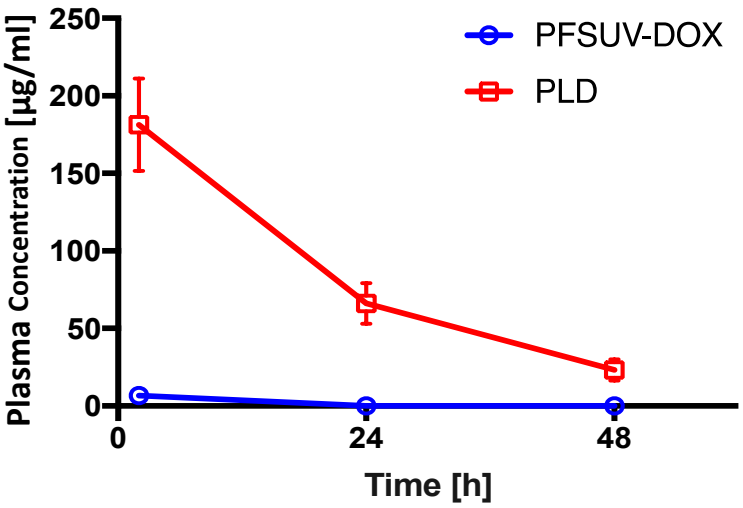

Figure 3-5 Plasma concentration of DOX post injection of PLD and PFLUVs-DOX. Data = mean ± SD (n=3)

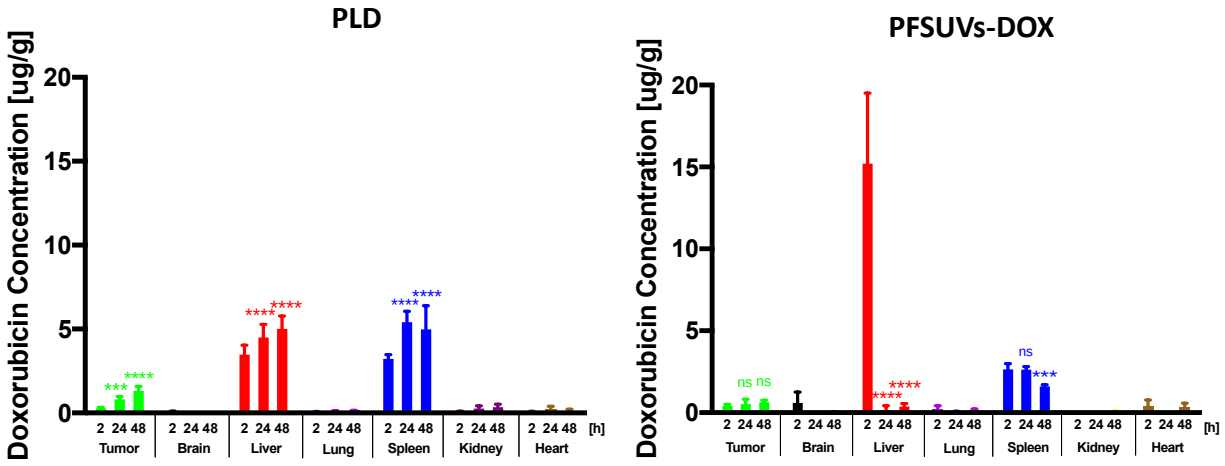

Figure 3-6 Biodistribution profiles of PLD and PFSUVs-DOX. Data = mean ± SD (n=3)

3.3.7 Liver uptake of PFSUVs-DOX

To examine what cells in the liver contributing to the uptake of PFSUVs-DOX, the liver was collected 2 h after injection, sectioned and imaged. As shown in Fig 3-7, significant DOX fluorescence was detected in both hepatocytes and sinusoidal cells.

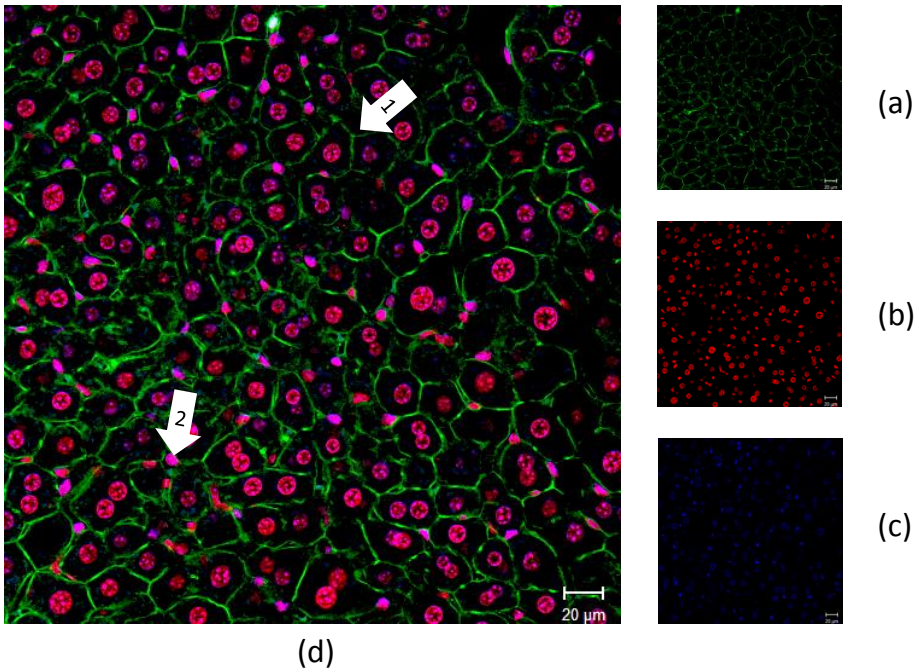

Figure 3-7 PFSUVs-DOX uptake by the liver. (a) Cell profile stained by Phalloidin; (b) Dox; (c) DAPI; (d) Merged. Arrow 1 shows hepatocyte; arrow 2 indicates Kupffer cell.

3.4 Discussion

PFSUVs-DOX were fabricated using microfluidics, and because of the relatively low solubility of cholesterol in ethanol, the produced PFSUVs were in very diluted and needed further concentration for in vivo studies. The ultrafiltration method was first used to concentrate PFSUVs-DOX, but it led to disruption of the particles possibly due to the collapse of the SUVs onto

the membrane by high centrifugation force. Therefore, the TFF system was utilized, allowing simultaneous ethanol removal, buffer exchange and particle concentration under gentle and controlled conditions. In the TFF system, the particle flow was in parallel with the diafiltration membrane, thus reducing the collapse of the particles onto the membrane.

The PLD was prepared using the standard thin-film hydration and membrane extrusion method, and even after extrusion through a 50-nm membrane, the size was slightly above 100 nm. The PLD formulation appeared to be flexible in changing the conformation to squeeze through the small pores during the extrusion and then rearrange back to the larger particles. On the other hand, PFSUVs were produced by microfluidics without membrane extrusion, but exhibited a small size (60-80 nm), a narrow PDI (<0.2). Our unpublished previous work showed that the size of the resulting particles could be manipulated by adjusting the microfluidic parameters, such as lipid concentration, ethanol/water ratio, mixing speed and mixing temperature. However, my thesis focused on comparing the innovative PFSUVs-DOX with PLD prepared using the standard methods, and we did not intend to fabricate PFSUVs with comparable formulation parameters as the PLD. PFSUVs-DOX were composed of neutral lipids and therefore, displayed a zeta potential value of -5 mV. DSPE-PEG2000 (~4 mol%) included in the PLD formulation contains one phosphate group and thus contributed to the anionic surface charged of PLD (ZP -25 mV). The PLD formulation exhibited increased loading capacity for DOX with a high D/L of 1/8, which was ~3-fold higher than that of PFSUVs-DOX. This could be due to an increased concentration of ammonium sulfate in the PLD relative to PFSUVs (250 mM vs. 120 mM). Our results indicated that the PFSUVs formulation could stably maintain an isotonic ammonium sulfate gradient (120 mM) for active loading and retention of

DOX. However, whether this formulation could keep a hypertonic ammonium gradient (i.e., 250 mM) for increased drug loading is yet to be investigated. To the best of our knowledge, it is the first report showing a drug could be actively loaded into and retained in a PFSUVs formulation (i.e., no drug leakage during 3-day incubation with 50% FBS). In previous studies, 50-80% of drug leakage from niosomal formulations was reported after 24-48 h incubation [(40)][38][(41)][39]. The low drug leakage from the PFSUVs-DOX could be explained by the stable DOX crystalline formation in the core and high cholesterol content that would grant high membrane rigidity to reduce drug permeation.

In the cellular uptake study, DOX was shown to rapidly penetrate the EMT6 cell membrane and bind with accumulated in the nucleus. Little cellular uptake was observed with the PLD because the surface PEGylation introduced steric hindrance to reduce the interaction with the cells. In the PFSUVs formulation, Tween80 also provided PEGylation to the particles and reduced the uptake by the EMT6 cells in the absence of serum. However, in the presence of serum, the PFSUVs-DOX uptake was increased by 2-fold. It has been shown that Tween80 attracted serum ApoE adsorption[40], which could be recognized by the low density lipoprotein (LDL) receptor to trigger receptor-mediated endocytosis.[41] More importantly, after 4 h of incubation in the presence of serum, DOX was detected in the nucleus of EMT6 cells treated with PFSUVs-DOX, suggesting significant intracellular delivery and release of the drug. The cellular uptake results translated well to the in vitro cytotoxicity data, wherein free DOX and PFSUVs-DOX displayed comparable potency against EMT6 cells, while PLD showed significantly reduced cytotoxicity.

The pharmacokinetics and biodistribution data of PLD were comparable as the previously reported PLD formulation[42, 43]. PLD displayed significantly prolonged plasma circulation and

selectively accumulated in the tumor, liver and spleen. Particularly in the tumor, the PLD uptake increased over time, which was consistent with the passive targeting mechanism [44]. Nanoparticles selectively extravasate into tumors through their leaky vasculature, a feature that does not exist in many normal tissues except the liver, spleen and bone marrow. This extravasation process is random and slow, so that prolonged blood circulation is required. The pharmacokinetic and biodistribution profiles of PFSUVs-DOX were distinctive from the PLD. PFSUVs-DOX was short-lived in the plasma and only a minimal DOX concentration could be detected in the plasma 2 h post injection. In the biodistribution results, it was shown that PFSUVs-DOX were largely taken up the by the liver and removed from the blood circulation. The uptake by the other examined tissues was only minimal, suggesting this formulation targeted the liver in high efficiency. Additionally, the drug was largely delivered to the hepatocyte rather than the Kupffer cells. Again, this could be explained by several factors. First, PFSUVs-DOX were 60-80 nm in size, which could easily pass the liver fenestrae (mean size ~ 100 nm) to reach the hepatocytes [45]. Second, the blood flow to the liver is high and this would bring a large dose of PFSUVs-DOX to the liver. Third, hepatocyte is known to overexpress LDL receptor[46] and the Tween80/ApoE/LDL-receptor mechanism described earlier would help the internalization of PFSUVs-DOX. The results indicated that this liver-targeted formulation may be used to deliver other drugs for treating liver diseases. It is also interesting to see that the liver uptake of DOX rapidly declined to the background 24 h post injection, which could be due to that DOX is a substrate for P-glycoprotein that is highly expressed in the hepatocyte and that DOX would be rapidly removed from the hepatocytes by the efflux pump. Similarly, DOX delivered by PFSUVs was detected in the brain 2 h post injection but rapidly cleared. The data could be

justified by the same reasons mentioned above that the brain endothelial cells (so called blood-brain barrier) overexpress LDL receptor and P-glycoprotein. Our data also showed that because there was no prolonged circulation of PFSUVs-DOX, the tumor accumulation did not increased over time. For both PLD and PFSUVs-DOX formulations, the heart uptake was little, which was supported by the strong association of DOX with the formulations in the presence of serum. Overall, the data indicated that PLD and PFSUVs-DOX behaved very differently in biological systems.

Chapter 4: Conclusion and future directions

In this study, we developed a novel PFSUV formulation (60-80 nm) with high cholesterol by microfluidic. This is the first time that a surfactant based formulation with cholesterol content over 80% has ever been reported. Even with this high cholesterol concentration, a bilayer structure was still observed by the cryo-TEM, allowing active loading procedure for DOX and a stable retention in the PFSUVs via an ammonium gradient. PFSUVs-DOX displayed significantly different profiles of pharmacokinetics and biodistribution compared to PLD, and were demonstrated to be hepatocyte-targeting in mice.

Using microfluidics method, we fabricated PFSUVs that have never been reported with potential to overcome a number of fabrication challenges in traditional niosomes, including difficulties in homogenous hydration and efficient membrane extrusion for size control. The lab will continue investigating how different microfluidic conditions will affect the characteristics (size, PDI, EE%) of PFSUVs and how these different formulations behave in biological systems such as cell culture and mice. In our latest research, we found that temperature can significantly affect the size and size distribution of PFSUV formulations. Our current work focuses on monitoring the stability of these different size PFSUVs.

It was thought that the phospholipid-free bilayer would be very leaky and would not maintain a loading gradient. However, the high cholesterol concentration can play a role to retain the gradient for active loading. Therefore, it is of interest to explore whether this formulation would be compatible with different loading gradients for active encapsulation of other drugs for various applications. In our previous study, a citric acid gradient (300 mM) was employed with the PFSUV

for DOX loading. This result suggested that PFSUVs exhibit significant potential for encapsulating different drugs via various loading gradients. Other loading gradients such as $Mn^{2+,}$ Cu^{2+}, Ca^{2+}, oligomers will be used to load a wide range of compounds that have been reported in the literature [47][48][49]to demonstrate the applicability of this delivery system. A few more control studies will be performed to test the Tween80/ApoE/LDL-receptor mechanism, including testing the effect of addition of ApoE in the serum free medium on cellular uptake and comparing the intra-liver uptake profiles of PFSUVs-DOX and PLD. Anti-LDL receptor antibody will also be used to further confirm that PFSUV's high uptake is related to LDL endocytosis pathway. To establish the medical potential of the PFSUVs formulation, a drug for treating a liver disease will be loaded into PFSUVs and the efficacy will be compared with the free drug. It would also be interesting to incorporate an imaging probe into the PFSUVs and explore the possibility of enhanced liver imaging. From Fig.3-7, it indicated that PFSUV-DOX also exhibited increased brain uptake, and it was reported that the LDL receptor mediated transcytosis has been utilized for drug delivery to the brain. We will continue optimizing the formulation to manipulate the physicochemical properties for improved brain delivery. Finally, as we discussed earlier, microfluidic system can introduce efficient cholesterol distribution in the nanoparticles, resulting in a formulation with improved stability. Therefore, other nonionic surfactants may be used to replace Tween80 to generate new formulations that may display different biodistribution profiles for different medical applications.

Reference

1. Mallick, S. and J.S. Choi, Liposomes: Versatile and Biocompatible Nanovesicles for Efficient Biomolecules Delivery. Journal of Nanoscience and Nanotechnology, 2014. 14(1): p. 755-765.
2. Han, H.D., B.C. Shin, and H.S. Choi, Doxorubicin-encapsulated thermosensitive liposomes modified with poly(N-isopropylacrylamide-co-acrylamide): Drug release behavior and stability in the presence of serum. European Journal of Pharmaceutics and Biopharmaceutics, 2006. 62(1): p. 110-116.
3. Jass, J., T. Tjärnhage, and G. Puu, From Liposomes to Supported, Planar Bilayer Structures on Hydrophilic and Hydrophobic Surfaces: An Atomic Force Microscopy Study. Biophysical Journal, 2000. 79(6): p. 3153-3163.
4. Xu, Q., Y. Tanaka, and J.T. Czernuszka, Encapsulation and release of a hydrophobic drug from hydroxyapatite coated liposomes. Biomaterials, 2007. 28(16): p. 2687-2694.
5. Bastiat, G., et al., Development of Non-Phospholipid Liposomes Containing a High Cholesterol Concentration. Langmuir, 2007. 23(14): p. 7695-7699.
6. Paré, C. and M. Lafleur, Formation of Liquid Ordered Lamellar Phases in the Palmitic Acid/Cholesterol System. Langmuir, 2001. 17(18): p. 5587-5594.
7. Moghassemi, S. and A. Hadjizadeh, Nano-niosomes as nanoscale drug delivery systems: An illustrated review. Journal of Controlled Release, 2014. 185: p. 22-36.
8. Fang, J.-Y., et al., Effect of liposomes and niosomes on skin permeation of enoxacin. International Journal of Pharmaceutics, 2001. 219(1): p. 61-72.
9. Manosroi, A., et al., Transdermal absorption enhancement through rat skin of gallidermin loaded in niosomes. International Journal of Pharmaceutics, 2010. 392(1): p. 304-310.
10. Manconi, M., et al., Niosomes as carriers for tretinoin: II. Influence of vesicular incorporation on tretinoin photostability. International Journal of Pharmaceutics, 2003. 260(2): p. 261-272.
11. Nagarajan, R., Molecular Packing Parameter and Surfactant Self-Assembly: The Neglected Role of the Surfactant Tail. Langmuir, 2002. 18(1): p. 31-38.
12. Khalil, R.A. and A.-h.A. Zarari, Theoretical estimation of the critical packing parameter of amphiphilic self-assembled aggregates. Applied Surface Science, 2014. 318: p. 85-89.
13. Lipshultz, S.E., et al., Late Cardiac Effects of Doxorubicin Therapy for Acute Lymphoblastic Leukemia in Childhood. New England Journal of Medicine, 1991. 324(12): p. 808-815.
14. Abdelkader, H., et al., Preparation of niosomes as an ocular delivery system for naltrexone hydrochloride: Physicochemical characterization. Die Pharmazie - An International Journal of Pharmaceutical Sciences, 2010. 65(11): p. 811-817.
15. Abdelkader, H., A.W.G. Alani, and R.G. Alany, Recent advances in non-ionic surfactant vesicles (niosomes): self-assembly, fabrication, characterization, drug delivery applications and limitations. Drug Delivery, 2014. 21(2): p. 87-100.

16. Abdelkader, H., U. Farghaly, and H. Moharram, Effects of surfactant type and cholesterol level on niosomes physical properties and in vivo ocular performance using timolol maleate as a model drug. Journal of Pharmaceutical Investigation, 2014. 44(5): p. 329-337.
17. Mokhtar, M., et al., Effect of some formulation parameters on flurbiprofen encapsulation and release rates of niosomes prepared from proniosomes. International Journal of Pharmaceutics, 2008. 361(1): p. 104-111.
18. Mashal, M., et al., Retinal gene delivery enhancement by lycopene incorporation into cationic niosomes based on DOTMA and polysorbate 60. Journal of Controlled Release, 2017. 254: p. 55-64.
19. Yadav, Proniosomal Gel: A provesicular approach for transdermal drug delivery. Der Pharmacia Lettre, 2010. 2(4).
20. Waddad, A.Y., et al., Formulation, characterization and pharmacokinetics of Morin hydrate niosomes prepared from various non-ionic surfactants. International Journal of Pharmaceutics, 2013. 456(2): p. 446-458.
21. Ojeda, E., et al., The influence of the polar head-group of synthetic cationic lipids on the transfection efficiency mediated by niosomes in rat retina and brain. Biomaterials, 2016. 77: p. 267-279.
22. M., H.V.R., et al., Dispersions of lamellar phases of non‐ionic lipids in cosmetic products. International Journal of Cosmetic Science, 1979. 1(5): p. 303-314.
23. Auda, S.H., et al., Niosomes as transdermal drug delivery system for celecoxib: in vitro and in vivo studies. Polymer Bulletin, 2016. 73(5): p. 1229-1245.
24. Budhiraja, A., Development and characterization of a novel antiacne niosomal gel of rosmarinic acid. Drug delivery. 22(6): p. 723-730.
25. Soliman, S.M., Novel non-ionic surfactant proniosomes for transdermal delivery of lacidipine: optimization using 2 factorial design and evaluation in rabbits. Drug delivery. 23(5): p. 1608-1622.
26. Li, Q., et al., Proniosome-derived niosomes for tacrolimus topical ocular delivery: In vitro cornea permeation, ocular irritation, and in vivo anti-allograft rejection. European Journal of Pharmaceutical Sciences, 2014. 62: p. 115-123.
27. Zeng, W., et al., Hyaluronic acid-coated niosomes facilitate tacrolimus ocular delivery: Mucoadhesion, precorneal retention, aqueous humor pharmacokinetics, and transcorneal permeability. Colloids and Surfaces B: Biointerfaces, 2016. 141: p. 28-35.
28. Gaafar, P.M.E., Preparation, characterization and evaluation of novel elastic nano-sized niosomes (ethoniosomes) for ocular delivery of prednisolone. Journal of liposome research. 24(3): p. 204-215.
29. Khalil, R.M., et al., Design and evaluation of proniosomes as a carrier for ocular delivery of lomefloxacin HCl. Journal of Liposome Research, 2017. 27(2): p. 118-129.
30. Maeda, H., et al., Tumor vascular permeability and the EPR effect in macromolecular therapeutics: a review. Journal of Controlled Release, 2000. 65(1): p. 271-284.
31. Uchegbu, I.F., Distribution, metabolism and tumoricidal activity of doxorubicin administered in sorbitan monostearate (Span 60) niosomes in the mouse. Pharmaceutical research, 1995. 12(7): p. 1019-1024.
32. Tagami, T., et al., A thermosensitive liposome prepared with a Cu2+ gradient demonstrates improved pharmacokinetics, drug delivery and antitumor efficacy. Journal of Controlled Release, 2012. 161(1): p. 142-149.

33. Chiu, G.N.C., et al., Encapsulation of doxorubicin into thermosensitive liposomes via complexation with the transition metal manganese. Journal of Controlled Release, 2005. 104(2): p. 271-288.
34. Jain, C.P. and S.P. Vyas, Preparation and characterization of niosomes containing rifampicin for lung targeting. Journal of Microencapsulation, 1995. 12(4): p. 401-407.
35. Baillie, A.J., The preparation and properties of niosomes-non-ionic surfactant vesicles. Journal of Pharmacy and Pharmacology. 37(12): p. 863-868.
36. Belliveau, N.M., et al., Microfluidic Synthesis of Highly Potent Limit-size Lipid Nanoparticles for In Vivo Delivery of siRNA. Molecular Therapy - Nucleic Acids, 2012. 1: p. e37.
37. Tagami, T., M.J. Ernsting, and S.-D. Li, Efficient tumor regression by a single and low dose treatment with a novel and enhanced formulation of thermosensitive liposomal doxorubicin. Journal of Controlled Release, 2011. 152(2): p. 303-309.
38. Uchegbu, I.F., et al., Distribution, Metabolism and Tumoricidal Activity of Doxorubicin Administered in Sorbitan Monostearate (Span 60) Niosomes in the Mouse. Pharmaceutical Research, 1995. 12(7): p. 1019-1024.
39. Uchegbu, I.F., The Activity of Doxorubicin Niosomes Against an c Cancer Cell Line and Three Mouse Tumour Models. Journal of drug targeting. 3(5): p. 399-409.
40. Kreuter, J., et al., Apolipoprotein-mediated Transport of Nanoparticle-bound Drugs Across the Blood-Brain Barrier. Journal of Drug Targeting, 2002. 10(4): p. 317-325.
41. Zhu, J.-Y., et al., Efficient nuclear drug translocation and improved drug efficacy mediated by acidity-responsive boronate-linked dextran/cholesterol nanoassembly. Biomaterials, 2015. 52: p. 281-290.
42. Vail, D.M., et al., Pegylated liposomal doxorubicin: Proof of principle using preclinical animal models and pharmacokinetic studies. Seminars in Oncology, 2004. 31: p. 16-35.
43. Gabizon, A., et al., Dose Dependency of Pharmacokinetics and Therapeutic Efficacy of Pegylated Liposomal Doxorubicin (DOXIL) in Murine Models. Journal of Drug Targeting, 2002. 10(7): p. 539-548.
44. Gabizon, A., H. Shmeeda, and Y. Barenholz, Pharmacokinetics of Pegylated Liposomal Doxorubicin. Clinical Pharmacokinetics, 2003. 42(5): p. 419-436.
45. Brown, M.S., Lipoprotein receptors in the liver. Control signals for plasma cholesterol traffic. The Journal of clinical investigation. 72(3): p. 743-747.
46. Pathak, R.K., et al., Tissue-specific sorting of the human LDL receptor in polarized epithelia of transgenic mice. The Journal of Cell Biology, 1990. 111(2): p. 347-359.
47. Cheung, Benny CL, et al. "Loading of doxorubicin into liposomes by forming Mn 2+-drug complexes." Biochimica et Biophysica Acta (BBA)-Biomembranes 1414.1 (1998):p. 205-216.
48. Ramsay, Euan, et al. "Transition metal-mediated liposomal encapsulation of irinotecan (CPT-11) stabilizes the drug in the therapeutically active lactone conformation." Pharmaceutical research 23.12 (2006): p. 2799-2808.
49. Gubernator, Jerzy. "Active methods of drug loading into liposomes: recent strategies for stable drug entrapment and increased in vivo activity." Expert opinion on drug delivery 8.5 (2011):p. 565-580.